

A NOVEL COMPRESSED SENSING BASED METHOD FOR SPACE TIME SIGNAL PROCESSING FOR AIRBORNE RADARS

Jing Liu^{*}, Chongzhao Han, Xianghua Yao, and Feng Lian

School of Electronics and Information Engineering, Xi'an Jiaotong University, Xi'an, P. R. China

Abstract—Space time adaptive processing (STAP) is a signal processing technique for detecting slowly moving targets using airborne radars. The traditional STAP algorithm uses a lot of training cells to estimate the space-time covariance matrix, which occupies large computer memory and is time-consuming. Recently, a number of compressed sensing based STAP algorithms are proposed to detect moving target in strong clutter situation. However, the coherence of the sensing matrix is not low due to the high resolution of the DOA (direction of arrival)-Doppler plane, which does not guarantee a good reconstruction of the sparse vector with large probability. Consequently, the direct estimation of the target amplitude may be unreliable using sparse representation when locating a moving target from the surrounding strong clutter. In this study, a novel method named similar sensing matrix pursuit is proposed to reconstruct the sparse radar scene directly based on the test cell, which reduces the computing complexity efficiently. The proposed method can efficiently cope with the deterministic sensing matrix with high coherence. The proposed method can estimate the weak elements (targets) as well as the prominent elements (clutter) in the DOA-Doppler plane accurately, and distinguish the targets from clutter successfully.

1. INTRODUCTION

A great deal of compressed sensing based methods have been applied to radar systems [1–9], which recover the target scene from fewer measurements than traditional methods. In [1], it is demonstrated that the compressed sensing can eliminate the need for matched filter

Received 31 March 2013, Accepted 22 May 2013, Scheduled 26 May 2013

* Corresponding author: Jing Liu (elelj20080730@gmail.com).

at the receiver and has the potential to reduce the required sampling rate. [2] presents an adaptive clutter suppression method for airborne random pulse repetition interval radar by using prior knowledge of clutter boundary in Doppler spectrum. [3] focuses on monostatic chaotic multiple-input-multiple-output (MIMO) radar systems and analyze theoretically and numerically the performance of sparsity-exploiting algorithms for the parameter estimation of targets at Low-SNR. In the context of synthetic aperture radar (SAR), [4–9] present compressed sensing based data acquisition and imaging algorithms.

STAP is a signal processing technique that was originally developed for detecting slowly moving targets using airborne radars [10–13]. It represents the simultaneous adaptive application of both Doppler filtering and spatial beamforming [14, 15], and allows the suppression of clutter that neither technique could individually address. While much of the early work in STAP focuses on the simplest case of side-looking uniform linear arrays (ULAs) operating monostatically, STAP techniques have also been applied to bistatic systems, conformal arrays, space-based systems, and other applications [16]. However, the traditional STAP algorithm uses a lot of training cells to estimate the space-time covariance matrix, which occupies large computer memory and is time-consuming.

In recent years, a number of compressed sensing based methods are proposed to detect unknown moving targets in strong clutter situation directly on the space-time data, which reduces the measurement data efficiently [17–20]. In [17], the entire radar scene, DOA-Doppler plane, is reconstructed using a compressed sensing based approach. In [18] the problem of clutter is addressed by applying a mask to the signal in the DOA-Doppler plane before penalizing. However, it is based on the assumption of known clutter ridge location. The work in [19] is a combination of the traditional STAP algorithm and compressed sensing. In [20], a new direct data domain approach using sparse representation (D3SR) is proposed to estimate the high-resolution space-time spectrum with only the test cell. However, the method assumes that the area where the targets locate is known in prior.

The classical model of compressed sensing, $\mathbf{y} = \mathbf{\Phi}\mathbf{x} + \mathbf{e}$, is adopted in the above work. The measurement vector \mathbf{y} represents the received echo signal snapshot from fixed range cell, and \mathbf{x} is the collection of the strength of the original transmitted signals (including targets, clutter or both) from the whole DOA-Doppler plane. \mathbf{e} denotes the measurement noise. The sensing matrix $\mathbf{\Phi}$ is comprised of Spatial-Doppler steering vectors in column, which is deterministic in nature. All the above work assumes that the sparse vector \mathbf{x} could be reconstructed based on the sensing matrix $\mathbf{\Phi}$ perfectly. However,

the coherence of the sensing matrix is not low due to the high resolution of the DOA-Doppler plane, which does not guarantee a good reconstruction of the sparse vector with large probability according to [21–26]. The simulation results in Section 3.5 in this paper show that large reconstruction error exists when relying on the original sensing matrix Φ .

In this study, a novel method named similar sensing matrix pursuit, is proposed to reconstruct the K -sparse signal based on the original deterministic sensing matrix. The proposed method consists of two parts: the off-line work and the online work. The goal of the off-line work is to construct a similar compacted sensing matrix with low coherence, which contains as much as possible information from the original sensing matrix. The online work begins when the measurements arrive, which consists of a rough estimation process and a refined estimation process. In the rough estimation process, an SP algorithm is used to find a rough estimate of the true support set, which contains the indices of the columns that contribute to the original sparse vector. Three kinds of structures of the estimated support set are considered, and three individual refined estimation processes are carried out under these three conditions respectively. From the simulation results, it can be seen that the proposed method obtains much better performance when coping with deterministic sensing matrix with high coherence compared with the SP and BP algorithms.

In this paper, we consider the application of detecting unknown moving targets in strong clutter situation using airborne radar system. Since the airborne radar scenario has a high CSR (clutter-signal-ratio, > 20 dB), the prominent elements of the spectral distribution focus along the clutter ridge in the DOA-Doppler plane. Therefore, it is reasonable to assume that the received data of the test cell is sparse in the DOA-Doppler plane [20]. The proposed similar sensing matrix pursuit method is then used to reconstruct the sparse signal representing the radar scene. From the simulation results, it can be seen that both the prominent elements (clutter) and the weak elements (targets) are recovered accurately in the reconstructed DOA-Doppler plane, and consequently the targets are distinguished from the clutter successfully. This is due to the reason that the proposed similar sensing matrix pursuit method can cope with the deterministic sensing matrix with high coherence efficiently.

The main contribution of this paper consists of the following three aspects: First, a novel method named similar sensing matrix pursuit is proposed to cope with the deterministic sensing matrix with large coherence. Secondly, a novel compressed sensing based method is utilized to detect multiple moving targets in strong clutter situation

directly on the space-time data and we need to know neither the clutter ridge location nor the target area. Thirdly, the proposed method uses only the data from the test cell, which reduces the computation burden efficiently.

The paper is organized as follows: Section 2 introduces a general space-time model for airborne radar system, which is represented in a compressed sensing framework. Our main contribution, the similar sensing matrix pursuit method, is introduced in Section 3, and the compressed sensing based multiple targets detection algorithm is introduced in Section 4. The simulation results are listed in Section 5, and the paper is summarized in Section 6.

2. A GENERAL SPACE-TIME MODEL AND ITS SPARSE REPRESENTATION

In this paper, we consider an airborne radar system which transmits K coherent pulse trains and samples the returns on ULAs consisting of N elements. For each pulse, it collects Q temporal samples from each element receiver, where each time sample corresponds to a range cell. The collection of samples for the q th range cell is represented by an $N \times K$ data matrix \mathbf{F} (snapshot) with elements $f(n, k)$ as,

$$\mathbf{F} = \begin{bmatrix} f(1, 1) & f(1, 2) & \dots & f(1, K) \\ f(2, 1) & f(2, 2) & \dots & f(2, K) \\ \vdots & \vdots & \ddots & \vdots \\ f(N, 1) & f(N, 2) & \dots & f(N, K) \end{bmatrix}. \quad (1)$$

A test cell is assumed to be comprised of target and clutter components. First, assuming D targets are observed in the far-field, the i th target is at a DOA angle of θ_i^t with Doppler frequency $f_{d_i}^t$. We can obtain an $NK \times 1$ complex vector \mathbf{y}_t as,

$$\mathbf{y}_t = \sum_{i=1}^D \beta(\theta_i^t, f_{d_i}^t) [\mathbf{s}_S(\theta_i^t) \otimes \mathbf{s}_T(f_{d_i}^t)], \quad (2)$$

where $\beta(\theta_i^t, f_{d_i}^t)$ is the reflection coefficient of the i th target, ' \otimes ' represents the Kronecker product of two vectors. The spatial steering vector $\mathbf{s}_S(\theta_i^t)$ and the Doppler filtering steering vector $\mathbf{s}_T(f_{d_i}^t)$ are represented by

$$\mathbf{s}_S(\theta_i^t) = \left[1, e^{j \frac{2\pi d}{\lambda} \sin \theta_i^t}, \dots, e^{j(N-1) \frac{2\pi d}{\lambda} \sin \theta_i^t} \right]^T \quad (3)$$

and,

$$\mathbf{s}_T(f_{d_i}^t) = \left[1, e^{j \frac{2\pi f_{d_i}^t}{f_r}}, \dots, e^{j(K-1) \frac{2\pi f_{d_i}^t}{f_r}} \right]^T, \quad (4)$$

where d is the distance between the elements of the arrays, and λ and f_r denote wavelength and pulse repetition frequency, respectively.

Besides the target components, there also exists clutter component \mathbf{y}_c , which can be considered as a collection of independent scatters as,

$$\mathbf{y}_c = \sum_{i=1}^{N_c} \beta(\theta_i^c, f_{d_i}^c) [\mathbf{s}_S(\theta_i^c) \otimes \mathbf{s}_T(f_{d_i}^c)], \quad (5)$$

where N_c is the number of clutter scatters. θ_i^c and $f_{d_i}^c$ are the DOA angle and Doppler frequency for the i th clutter scatter respectively, and $\beta(\theta_i^c, f_{d_i}^c)$ is the reflection coefficient. $\mathbf{s}_S(\theta_i^c)$ and $\mathbf{s}_T(f_{d_i}^c)$ represent the spatial steering vector and the Doppler filtering steering vector respectively.

Using the above modeling, the $NK \times 1$ complex vector of the test cell can be modeled as

$$\mathbf{y}_{\text{test}} = \mathbf{y}_t + \mathbf{y}_c + \mathbf{e}, \quad (6)$$

where \mathbf{e} is an $NK \times 1$ complex Gaussian noise vector.

In this paper, compressed sensing is used to estimate the spectral distributions of the targets and clutter scatters in the DOA-Doppler plane. To do so, the DOA-Doppler plane is divided into $V \times L$ square grids, where V and L denote the number of rows (for Doppler frequency) and columns (for DOA angle), respectively. Each grid is with the same size $\Delta\theta \times \Delta f_d$. Grid (i, j) represents a DOA angle of θ_i ($\theta_0 + (i - 1)\Delta\theta$) and a Doppler frequency of f_{d_j} ($f_{d_0} + (i - 1)\Delta f_d$), where θ_0 and f_{d_0} represent the initial DOA angle and initial Doppler frequency. All the grids in the DOA-Doppler plane are mapped into a 2-D vector \mathbf{x}_{test} with the j th column put at the end of the $(j - 1)$ th column.

Since the airborne radar scene has a high CSR (> 20 dB), the significant elements of the spectral distribution focus along the clutter ridge in the DOA-Doppler plane. Therefore, it is reasonable to assume that the received data of the test cell is sparse in the DOA-Doppler plane [20]. A small number of grids are occupied by the targets and clutter scatters in the DOA-Doppler plane, and \mathbf{x}_{test} is a sparse vector.

Based on the above derivation, a system for the test cell is built in a compressed sensing framework as in (7),

$$\mathbf{y}_{\text{test}} = \Phi \mathbf{x}_{\text{test}} + \mathbf{e}. \quad (7)$$

Φ is a sensing matrix with dimension $NK \times VL$, which is defined as $\Phi = [\varphi_1 \ \varphi_2 \ \dots \ \varphi_{VL}]$ in columns. The $((i - 1) \cdot L + j)$ th column of Φ is defined as follows,

$$\varphi_{(i-1) \cdot L + j} = \mathbf{s}_S(\theta_i) \otimes \mathbf{s}_T(f_{d_j}). \quad (8)$$

The sensing matrix Φ is with high coherence since V and D are set large values to obtain a high resolution of the DOA-Doppler plane.

Though in (7) the radar vectors and matrices are complex valued in contrary to the original compressed sensing environment, it is easy to transfer it to real variables according to [28, 29].

For simplicity, (7) is rewritten in a classical format in compressed sensing with subscripts removed.

$$\mathbf{y} = \Phi \mathbf{x} + \mathbf{e}. \quad (9)$$

3. THE PROPOSED SIMILAR SENSING MATRIX PURSUIT ALGORITHM

In the recently proposed compressed sensing based STAP algorithms [17–20], it is assumed that the sparse vector \mathbf{x} could be reconstructed perfectly based on the sensing matrix Φ . However, the coherence of the sensing matrix is not low due to the high resolution of the DOA-Doppler plane, which does not guarantee a good reconstruction of the sparse vector with large probability according to [21–26]. Consequently, the direct estimation of the target amplitude may be unreliable using sparse representation when locating a moving target from the surrounding strong clutter. In [20], only the prominent elements (clutter) are extracted from the sparse radar scene, and an additional adaptive filter is used to suppress the clutter to identify the target. The simulation results in Section 3.5 also show that large reconstruction error exists when relying on the sensing matrix Φ .

In this study, a novel method named similar sensing matrix pursuit is proposed to reconstruct the sparse vector \mathbf{x} representing the sparse radar scene. The proposed method can efficiently cope with the deterministic sensing matrix Φ with high coherence. As a result, the proposed method can estimate the weak elements (targets) as well as the prominent elements (clutter) accurately, and distinguish the targets from clutter successfully in the DOA-Doppler plane.

This section mainly introduces the proposed similar sensing matrix pursuit algorithm. First, the key component of the proposed algorithm, the similar compacted sensing matrix is introduced in Section 3.1, and the whole algorithm is introduced in Section 3.2. The convergence analysis and complexity analysis of the proposed algorithm are provided in Sections 3.3 and 3.4, respectively. Finally, a simple example is provided to compare the reconstruction performance of the proposed method with the basis pursuit (BP) and SP algorithms, which are commonly adopted by compressed sensing based works.

3.1. Construction of the Similar Compacted Sensing Matrix

The construction process of the similar compacted sensing matrix is based on the similarity analysis of the original sensing matrix. In this paper, similarity is defined as the absolute and normalized inner product between any two different columns in the original sensing matrix Φ , as

$$\lambda(\varphi_i, \varphi_j) = \frac{|\varphi_i^T \varphi_j|}{\|\varphi_i\| \cdot \|\varphi_j\|}, \quad 1 \leq i, j \leq N \text{ and } i \neq j. \quad (10)$$

It can be seen that coherence is the largest similarity among the columns of a matrix. Equation (10) represents a fundamental quantity in compressed sensing [21–26]. Here it is named as similarity to introduce the proposed algorithm properly. It can be seen that any two columns with large similarity value are coherent with each other, and vice versa. Therefore, the similarity can be used to distinguish the coherent columns from the incoherent columns of the original sensing matrix.

A different way to understand similarity and coherence are by considering the Gram matrix \mathbf{G} which is defined as [23],

$$\mathbf{G} = \tilde{\Phi}^T \tilde{\Phi}, \quad (11)$$

where $\tilde{\Phi}^T$ is the normalized sensing matrix obtained from the original sensing matrix with each column normalized. The off-diagonal entries in \mathbf{G} are the similarity values defined in (10). The coherence is the off-diagonal entry with the largest magnitude.

A threshold T_1 is set properly to distinguish the highly coherent columns from the incoherent columns as follows. For each calculated similarity value, $\{\lambda(\varphi_i, \varphi_j), i = 1, \dots, N, j = 1, \dots, N, i \neq j\}$, if $\lambda(\varphi_i, \varphi_j)$ is larger than T_1 , the columns i and j are added to the set of highly coherent columns. The remaining columns that do not belong to the set of highly coherent columns form the set of incoherent columns. Fig. 1 shows the classification results in a similarity plane, where the incoherent columns and the highly coherent columns are indicated by black circles and black squares respectively. In the similarity plane, the distance between any two columns (φ_i, φ_j) is defined as the similarity distance $d_{similar}$, which is inversely proportional to the similarity value $\lambda(\varphi_i, \varphi_j)$, as

$$d_{similar}(\varphi_i, \varphi_j) = K_s / \lambda(\varphi_i, \varphi_j), \quad (12)$$

where K_s is a constant. Therefore the closer the two columns locate in the similarity plane, the more similar they are (with larger similarity).

Figure 1 also shows that any two highly coherent columns may not be close to each other (coherent with each other) in the similarity

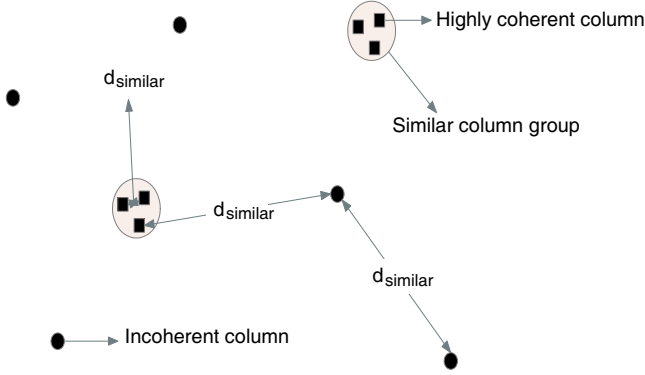


Figure 1. Classification results in a similarity plane.

plane. The highly coherent columns are then further divided into a set of similar column groups (indicated by large circles in Fig. 1) to ensure that the highly coherent columns in a similar column group are similar with each other. Moreover, the similar column groups are with the following property.

3.1.1. Property 1

For any two similar column groups, which are defined as $\Gamma^1 = \{\alpha_1, \dots, \alpha_N\}$ and $\Gamma^2 = \{\beta_1, \dots, \beta_M\}$, the similarity between any two columns from these two different similar column groups, e.g., $\alpha_i \in \Gamma^1$ and $\beta_j \in \Gamma^2$, is no larger than T_1 , as

$$\lambda(\alpha_i, \beta_j) \leq T_1, \quad \alpha_i \in \Gamma^1 \text{ and } \beta_j \in \Gamma^2, \quad (13)$$

while the similarity between any two columns in a single similar column group (e.g., Γ^1) is larger than a threshold T_2 , as

$$\lambda(\alpha_i, \alpha_j) > T_2, \quad \alpha_i, \alpha_j \in \Gamma^1 \text{ and } i \neq j. \quad (14)$$

Property 1 stipulates that any column in one specific similar column group is highly coherent with other columns inside the same group, while incoherent with any column outside the group (including the highly coherent columns in other similar column groups, and incoherent columns). This is reflected from Fig. 1 that any column in one large circle (similar column group) is very close to other columns inside the circle, while far apart from any column outside the circle. Therefore, any column in one specific similar column group represents the characteristics of other columns in the same group. In this paper, we consider reducing the original sensing matrix to a similar compacted sensing matrix by drawing a column from each similar column group, while keeping the incoherent columns unchanged in the new sensing

matrix. The newly built similar compacted sensing matrix contains as much as possible information from the original sensing matrix. And at the same time, it is with low coherence, which guarantees perfect reconstruction of a sparse vector with large probability. Next, the construction process of the similar compacted sensing matrix is briefly introduced.

3.1.2. Construction of the Similar Compacted Sensing Matrix

The set of highly coherent columns and the set of incoherent columns are denoted by $\mathbf{S}_{\text{hc}} = \{\boldsymbol{\nu}^1, \boldsymbol{\nu}^2, \dots, \boldsymbol{\nu}^{N_{\text{hc}}}\}$ and $\mathbf{S}_{\text{ic}} = \{\boldsymbol{\zeta}^1, \boldsymbol{\zeta}^2, \dots, \boldsymbol{\zeta}^{N_{\text{ic}}}\}$, respectively. N_{hc} is the number of highly coherent columns, and N_{ic} is the number of incoherent columns with $N_{\text{hc}} + N_{\text{ic}} = N$. The set of highly coherent columns \mathbf{S}_{hc} is further divided into D similar column groups, $\{\boldsymbol{\Gamma}^1, \boldsymbol{\Gamma}^2, \dots, \boldsymbol{\Gamma}^i, \dots, \boldsymbol{\Gamma}^D\}$. We assume that $M < D < N$. Each similar column group contains more than one highly coherent columns, e.g., $\boldsymbol{\Gamma}^i = \{\gamma_{N_{\Gamma^i}}^i, \dots, \gamma_1^i\}$, where N_{Γ^i} indicates the number of columns in $\boldsymbol{\Gamma}^i$. Each similar column group is condensed to a single column. Here we just select a column from each similar column group randomly considering that the columns in one group are highly coherent and very similar to each other. We obtain a similar compacted sensing matrix by combining the condensed columns and the incoherent columns, as $\boldsymbol{\Psi} = [\gamma_C^1, \gamma_C^2, \dots, \gamma_C^i, \dots, \gamma_C^D, \boldsymbol{\zeta}^1, \boldsymbol{\zeta}^2, \dots, \boldsymbol{\zeta}^{N_{\text{ic}}}]$, where γ_C^i denotes a condensed column from $\boldsymbol{\Gamma}^i$. We have the following propositions for the similar compacted sensing matrix.

3.1.3. Proposition 1

The coherence of the similar compacted sensing matrix is less than or equal to T_1 .

Proof: According to Property 1, the similarity between any two condensed columns is no larger than T_1 . Moreover, from the division process of the coherent columns and the incoherent columns, the similarity between any two incoherent columns, or between a condensed column and a incoherent column, is no larger than T_1 . As a result, the similarity between any two columns of the similar compacted sensing matrix is no larger than T_1 . Therefore, the coherence of the similar compacted sensing matrix, which is the largest similarity, is less than or equal to T_1 .

3.1.4. Proposition 2

[26, 30] Let the signal \mathbf{x} be a K -sparse vector and write $\mathbf{y} = \Phi\mathbf{x} + \mathbf{e}$. Denote $\gamma = \|\mathbf{e}\|_2$. Suppose that $K \leq (1/\mu(\Phi) + 1)/4$ and $\epsilon \geq \gamma$ in (15).

$$\hat{\mathbf{x}} = \arg \min_{\mathbf{x} \in \mathbb{R}^N} \|\mathbf{x}\|_1 \text{ subject to } \|\mathbf{y} - \Phi\mathbf{x}\|_2 \leq \epsilon \quad (15)$$

Then the output $\hat{\mathbf{x}}$ of (15) has error bounded by

$$\|\mathbf{x} - \hat{\mathbf{x}}\|_2 \leq \frac{\gamma + \epsilon}{\sqrt{1 - \mu(\Phi)(4K - 1)}}, \quad (16)$$

where $\mu(\Phi)$ denotes the coherence of the sensing matrix Φ . The output $\hat{\mathbf{x}}$ of the OMP algorithm with halting criterion $\|\mathbf{r}\|_2 \leq \gamma$ has error bounded by

$$\|\mathbf{x} - \hat{\mathbf{x}}\|_2 \leq \frac{\gamma}{\sqrt{1 - \mu(\Phi)(4K - 1)}}, \quad (17)$$

provided that $\gamma \leq A(1 - \mu(\Phi)(2K - 1))/2$ for OMP, with A being a positive lower bound on the magnitude of the nonzero entries of \mathbf{x} .

3.1.5. Proposition 3: Setting of the Threshold T_1

In order to guarantee a perfect reconstruction of the sparse vector with large probability, the threshold T_1 should satisfy (18) according to Propositions 1 and 2.

$$T_1 \leq 1/(4K - 1) \quad (18)$$

In this paper the threshold T_1 is set as $T_1 = 1/(4K - 1)$. However, small T_1 will result in a large number of highly coherent columns. While the restrict selection of T_1 is true from a worst-case standpoint, it turns out that the coherence as defined previously does not do justice to the actual behavior of sparse representations and pursuit algorithms' performance. Thus, if we relax our expectations and allow a small fraction of failed reconstructions, then values of substantially beyond the above bound are still leading to successful compressed sensing [31]. In this work, the threshold T_1 is set as 0.4 in the simulation settings. Meanwhile, the threshold T_2 should be set large enough to ensure that the columns in a similar column group are highly coherent (similar) with each other. Here the threshold T_2 is set as $T_2 = 0.9$.

3.2. The Similar Sensing Matrix Pursuit Algorithm

In this paper, a new algorithm named similar sensing matrix pursuit, is used to cope with the problem induced by the highly coherent columns. Firstly, the original sensing matrix is transformed to a similar

compacted sensing matrix based on similarity analysis. The similar compacted sensing matrix is with low coherence, which guarantees a perfect reconstruction of the sparse vector with large probability. An OMP-type method (SP algorithm) is then used to find a rough estimate of the true support set based on the similar compacted sensing matrix and the measurement vector, which contains the indices of the columns contributing to the original sparse vector. The contributing columns may include the incoherent columns and the condensed columns. Since a condensed column is selected from a similar column group randomly, we can only obtain the indices of the contributing similar column groups. From the rough estimation process, we can not decide the real contributing columns in the contributing similar column groups. Next, a refined estimation process is adopted to provide equal opportunities to all the columns in the contributing similar column groups. All the combinations of the columns in the contributing similar column groups and the contributing incoherent columns are listed, with each combination forming a candidate support set. Accordingly, we can obtain a candidate estimate of the original sparse vector using least square algorithm based on each candidate support set [23, 27]. Finally, we can find the estimated sparse vector matching the residual best.

The proposed method consists of off-line work and online work. The off-line work majors in the construction of the similar compacted sensing matrix. The online work consists of a rough estimation process and a refined estimation process. The main sparse reconstruction work is carried out in the rough estimation process, where the SP algorithm is used to find a rough estimate of the true support set. And the refined estimation process is a combinational searching work among the candidate support sets for the one matching the true support set best.

The estimated support set may only include the indices of the contributing condensed columns or the contributing incoherent columns, besides containing both of them. Three individual refined estimation processes are carried out under the above three conditions. Under the first condition, the true nonzero entries of the original sparse vector drop in a number of similar column groups. All the combinations of the columns in the contributing similar column groups are listed with each combination forming a candidate support set. A candidate estimate of the original sparse vector is obtained based on each candidate support set. Finally, we can find the estimated sparse vector matching the residual best. Under the second condition when the contributing columns include the incoherent columns only, the nonzero entries are easily identified since the compressed sensing method can clearly identify the entries corresponding to the incoherent

columns of the sensing matrix. Finally, the combination of the two methods from the first and the second condition can be used to estimate the original sparse vector under the third condition. The detailed procedure of the proposed algorithm is listed in the following.

3.2.1. Algorithm 1: The Similar Sensing Matrix Pursuit Algorithm

Input: Sensing matrix Φ , measurement vector \mathbf{y}

Output: The estimated signal $\hat{\mathbf{x}}_{\mathbf{O}}$

- (i) Construction of the Similar Compacted Sensing Matrix. The process is same with that in Section 3.1.
- (ii) Rough Estimation. The SP algorithm is used to find a rough estimate of the true support set based on the measurement vector \mathbf{y} and the similar compacted sensing matrix Ψ . The estimated support set is represented as, $\hat{\mathbf{a}} = \{\hat{a}^1, \hat{a}^2, \dots, \hat{a}^K\}$, where K is the sparsity level of the original K -sparse vector. The estimated support set $\hat{\mathbf{a}}$ contains the indices of the condensed columns or the indices of the incoherent columns, or both, which contribute to the original sparse vector.
- (iii) Refined Estimation. Three individual refined estimation processes are carried out under the following three conditions.
 - (a) $\hat{\mathbf{a}}$ contains the indices of the condensed columns only.
 - (1) The estimated support set $\hat{\mathbf{a}}$ is represented as $\hat{\mathbf{a}} = \{\hat{a}^1(\gamma_C^i), \hat{a}^2(\gamma_C^j), \dots, \hat{a}^K(\gamma_C^l)\}$, where $\hat{a}^1(\gamma_C^i)$ indicates that the first element of $\hat{\mathbf{a}}$ corresponds to γ_C^i , the index of the i th condensed column. Accordingly, we can obtain a set $\hat{\mathbf{b}}$ containing the indices of K similar column groups corresponding to $\hat{\mathbf{a}}$, as $\hat{\mathbf{b}} = \{\Gamma^i, \Gamma^j, \dots, \Gamma^l\}$. The indices of all the columns in the selected similar column groups in $\hat{\mathbf{b}}$ are listed and form a final set $\hat{\mathbf{f}}$ as, $\hat{\mathbf{f}} = \{\gamma_1^i, \dots, \gamma_{N_{\Gamma^i}}^i, \dots, \gamma_1^j, \dots, \gamma_{N_{\Gamma^j}}^j, \dots, \gamma_1^l, \dots, \gamma_{N_{\Gamma^l}}^l\}$. We assume that the total number of the indices in $\hat{\mathbf{f}}$ is H .
 - (2) Refined Estimation. List C_H^K combinations based on the column indices in $\hat{\mathbf{f}}$, and each combination forms a candidate support set, e.g., the p th candidate support set is represented as $\Upsilon_{\mathbf{p}} = \{\Upsilon_p^1(\gamma_1^i), \Upsilon_p^2(\gamma_1^j), \dots, \Upsilon_p^K(\gamma_1^l)\}$, $p = 1, 2, \dots, N_{co}$, where $\Upsilon_p^1(\gamma_1^i)$ indicates the first element of $\Upsilon_{\mathbf{p}}$ corresponding to γ_1^i , and N_{co} indicates the total number of combinations. The proposed algorithm then solves a least square problem to approximate the

nonzero entries of the original sparse vector on each candidate support set ($\Upsilon_p, p = 1, 2, \dots, N_{co}$), and sets other entries as zero, resulting in an estimate of the original sparse vector, $\hat{\mathbf{x}}^P$ [23, 27]. We can obtain the estimate $\hat{\mathbf{x}}^P$ as,

$$\hat{\mathbf{x}}_{\Upsilon^P}^P = \Phi_{\Upsilon^P}^\dagger \mathbf{y}, \quad (19)$$

$$\hat{\mathbf{x}}_{\{1,2,\dots,N\}-\Upsilon^P}^P = 0, \quad (20)$$

where \dagger indicates pseudo-inverse operation. The matrix Φ_{Υ^P} consists of the columns of Φ with indices $i \in \Upsilon^P$, $\hat{\mathbf{x}}_{\Upsilon^P}^P$ is composed of the entries of $\hat{\mathbf{x}}^P$ indexed by $i \in \Upsilon^P$, and $\hat{\mathbf{x}}_{\{1,2,\dots,N\}-\Upsilon^P}^P$ is composed of the entries of $\hat{\mathbf{x}}^P$ indexed by $i \in \{1, 2, \dots, N\} - \Upsilon^P$ [27].

- (3) Final Estimate. Among the obtained estimates $\{\hat{\mathbf{x}}^1, \hat{\mathbf{x}}^2, \dots, \hat{\mathbf{x}}^P, \dots, \hat{\mathbf{x}}^{N_{co}}\}$, find the estimate with the least residual, $\hat{\mathbf{x}}_{\min}$, and set $\hat{\mathbf{x}}_{\min}$ as the output estimated signal.

$$\hat{\mathbf{x}}_O = \hat{\mathbf{x}}_{\min} \quad (21)$$

- (b) $\hat{\mathbf{a}}$ contains the indices of the incoherent columns only.

- (1) The estimated support set $\hat{\mathbf{a}}$ can be represented as $\hat{\mathbf{a}} = \{\hat{a}^1(\zeta^i), \hat{a}^2(\zeta^j), \dots, \hat{a}^K(\zeta^l)\}^T$, where $\hat{a}^1(\zeta^i)$ indicates that the first element of $\hat{\mathbf{a}}$ corresponds to ζ^i , the i th incoherent column. The estimated support set $\hat{\mathbf{a}}$ equals the true support set of the original K -sparse vector due to the incoherence between the contributing incoherent columns.
- (2) Estimation. We can obtain the estimate of the original sparse vector using least square algorithm [23, 27] based on the true support set $\hat{\mathbf{a}}$, as

$$\hat{\mathbf{x}}_{\hat{\mathbf{a}}} = \Phi_{\hat{\mathbf{a}}}^\dagger \mathbf{y}, \quad (22)$$

$$\hat{\mathbf{x}}_{\{1,2,\dots,N\}-\hat{\mathbf{a}}} = 0. \quad (23)$$

- (3) Final Estimate.

$$\hat{\mathbf{x}}_O = \hat{\mathbf{x}} \quad (24)$$

- (c) $\hat{\mathbf{a}}$ contains the indices of both the condensed columns and the incoherent columns.

- (1) The estimated support set $\hat{\mathbf{a}}$ is represented as $\hat{\mathbf{a}} = \{\hat{a}^1(\gamma_C^i), \dots, \hat{a}^V(\gamma_C^j), \hat{a}^{V+1}(\zeta^k), \dots, \hat{a}^K(\zeta^l)\}$, where $\{\hat{a}^1(\gamma_C^i), \dots, \hat{a}^V(\gamma_C^j)\}$ correspond to V selected condensed columns, and $\{\hat{a}^{V+1}(\zeta^k), \dots, \hat{a}^K(\zeta^l)\}$ correspond

to K - V selected incoherent columns. Accordingly, we can obtain a set $\hat{\mathbf{b}}$ containing the indices of V similar column groups corresponding to $\{\hat{a}^1(\gamma_C^i), \dots, \hat{a}^V(\gamma_C^j)\}$, as $\hat{\mathbf{b}} = \{\Gamma^i, \dots, \Gamma^j\}$. The indices of all the columns in the selected similar column groups in $\hat{\mathbf{b}}$ are listed and form a final set $\hat{\mathbf{f}}$ as, $\hat{\mathbf{f}} = \{\gamma_1^i, \dots, \gamma_{N_{\Gamma^i}}^i, \dots, \gamma_1^j, \dots, \gamma_{N_{\Gamma^j}}^j\}$. We assume that the total number of the indices in $\hat{\mathbf{f}}$ is H .

- (2) Refined Estimation. List C_H^V combinations based on the column indices in $\hat{\mathbf{f}}$, and the p th combination can be represented as $\mathbf{r}_p = \{\gamma_1^i, \dots, \gamma_1^j\}$, $p = 1, 2, \dots, N_{cb}$, where N_{cb} indicates the total number of combinations. Each combination together with all the selected incoherent columns, $\{\zeta^k, \dots, \zeta^l\}$, forms a candidate support set. The p th candidate support set is represented as $\Upsilon_p = \{\Upsilon_p^1(\gamma_1^i), \dots, \Upsilon_p^V(\gamma_1^j), \Upsilon_p^{V+1}(\zeta^k), \dots, \Upsilon_p^K(\zeta^l)\}$, $p = 1, 2, \dots, N_{cb}$. The proposed algorithm then solves a least square problem to approximate the nonzero entries of the original sparse vector on each candidate support set (Υ_p , $p = 1, 2, \dots, N_{cb}$), and sets other entries as zero, resulting in an estimate of the original sparse vector, $\hat{\mathbf{x}}^p$ [23, 27]. We can obtain the estimate $\hat{\mathbf{x}}^p$ as,

$$\hat{\mathbf{x}}_{\Upsilon_p}^p = \Phi_{\Upsilon_p}^\dagger \mathbf{y}, \quad (25)$$

$$\hat{\mathbf{x}}_{\{1,2,\dots,N\}-\Upsilon_p}^p = 0. \quad (26)$$

- (3) Final Estimate. Among the obtained estimates $\{\hat{\mathbf{x}}^1, \hat{\mathbf{x}}^2, \dots, \hat{\mathbf{x}}^p, \dots, \hat{\mathbf{x}}^{N_{cb}}\}$, find the estimate with the least residual, $\hat{\mathbf{x}}_{\min}$, and set $\hat{\mathbf{x}}_{\min}$ as the output estimated signal.

$$\hat{\mathbf{x}}_O = \hat{\mathbf{x}}_{\min} \quad (27)$$

3.3. Convergence Analysis

The original sensing matrix is transformed to a similar compacted sensing matrix by condensing each similar column group to a condensed column and keeping the incoherent columns unchanged. The obtained similar compacted sensing matrix is with low coherence, which guarantees perfect reconstruction of the sparse vector with large probability according to Propositions 1 and 3. The SP algorithm is then used to find a rough estimate of the true support set, $\hat{\mathbf{a}}$, based on the measurement vector \mathbf{y} and the similar compacted sensing matrix Ψ . The rough estimate of the true support set, $\hat{\mathbf{a}}$, gives correct positions

of the nonzero entries corresponding to the contributing columns due to the incoherence between any two columns of the similar compacted sensing matrix. The estimated support set $\hat{\mathbf{a}}$ may contain the indices of the condensed columns or the indices of the incoherent columns, or both, which contribute to the original sparse vector. Three individual refined estimation processes are then carried out under these three conditions. And the convergence analysis are also based on these three conditions as follows.

- (i) $\hat{\mathbf{a}}$ contains the indices of the condensed columns only.

The rough estimate of the true support set, $\hat{\mathbf{a}}$, gives correct positions of the nonzero entries corresponding to the contributing condensed columns according to Propositions 1 and 3. They are the indices of the similar column groups contributing to the original sparse vector. In the refined estimation process, the combinations of all the columns in the contributing similar column groups are listed out as the candidate support sets, and the true support set is among them. Based on each candidate support set, we can obtain an estimate of the original sparse vector using least square algorithm [23, 27]. And finally we can get the estimated signal which matches the residual best. The estimated signal is with the error bounded by (17) according to Proposition 2.

- (ii) $\hat{\mathbf{a}}$ contains the indices of the incoherent columns only.

In this condition, the estimated support set $\hat{\mathbf{a}}$ equals the true support set of the original K -sparse vector due to the incoherence between the contributing incoherent columns. We can obtain the estimate of the original sparse vector using least square algorithm [23, 27] based on the true support set $\hat{\mathbf{a}}$. The estimated signal is with the error bounded by (17) according to Proposition 2.

- (iii) $\hat{\mathbf{a}}$ contains the indices of both the condensed columns and the incoherent columns.

The rough estimate of the true support set, $\hat{\mathbf{a}}$, gives correct positions of the nonzero entries corresponding to the contributing condensed columns and the contributing incoherent columns according to Propositions 1 and 3. So we can find the contributing similar column groups and the contributing incoherent columns. The combinations from the columns of the contributing similar column groups, together with the contributing incoherent columns form a number of candidate support sets, and the true support set is among them. Based on each candidate support set, we can obtain an estimate of the original sparse vector using least square algorithm [23, 27]. And finally we can get the estimated signal which matches the residual best. The estimated signal is with the

error bounded by (17) according to Proposition 2.

3.4. Complexity Analysis

The proposed approach consists of off-line work and online work. The off-line work transforms the original sensing matrix to a similar compacted sensing matrix based on similarity analysis. The computation complexity mainly focuses on the computation of the similarity between any two columns of the original sensing matrix, which is of the order of $O(\frac{(N-1)N}{2}M)$.

The online work begins when the measurements arrive, which consists of the rough and refined estimation processes. In the rough estimation process, an SP algorithm is used to find a rough estimate of the true support set, $\hat{\mathbf{a}}$, based on the measurement vector \mathbf{y} and the similar compacted sensing matrix Ψ . The computation complexity of the rough estimation process is same with that of the SP algorithm.

The estimated support set $\hat{\mathbf{a}}$ contains the indices of the condensed columns or the indices of the incoherent columns, or both, which contribute to the original sparse vector. Three individual refined estimation processes are carried out under the above conditions. And the complexity analysis will be based on these three conditions respectively.

- (i) $\hat{\mathbf{a}}$ contains the indices of the condensed columns only.

In the refined estimation, C_H^K combinations of all the columns in the contributing similar column groups are listed out as the candidate support sets. Based on each candidate support set, the nonzero entries of the estimated sparse vector are calculated using least square algorithm. So the computation cost is of the order of $C_H^K \times O(LS)$, where $O(LS)$ indicates the order of the computation cost for the least square algorithm.

- (ii) $\hat{\mathbf{a}}$ contains the indices of the incoherent columns only.

The rough estimate of the true support set, $\hat{\mathbf{a}}$, gives correct positions of the entries corresponding to the incoherent columns, based on which we can reconstruct the original sparse vector using the least square algorithm. So the computation cost is of the order of $O(LS)$.

- (iii) $\hat{\mathbf{a}}$ contains the indices of both the condensed columns and the incoherent columns.

We assume that $\hat{\mathbf{a}}$ contains the indices of V contributing similar column groups and the indices of $K - V$ incoherent columns. The combinations from the columns of the contributing similar column groups, together with the contributing incoherent columns form a

number of candidate support sets, among which we can find the true one that matches the residual best. So the computation cost is of the order of $C_H^V \times O(LS)$.

3.5. A Simple Example

In this example, the proposed similar sensing matrix pursuit algorithm is compared with the SP and BP algorithms in reconstructing both binary zero-one and Gaussian sparse signals. The length of the sparse vector (N) and the measurement vector (M) are set as 20 and 10 respectively. A signal sparsity level K is chosen such that $K \leq M/2$. A support set s of size K is selected uniformly at random, and the original sparse vector is chosen as either Gaussian signal or zero-one signal [27]. In the experiments, the BP algorithm uses the default settings (refer to SparseLab [32]), and the SP algorithm uses the parameters given in [27]. Five hundred Monte Carlo simulations are performed for each fixed value of K (size of the support set). The reconstruction is considered to be exact when the l_2 norm of the difference between the original signal \mathbf{x} and the reconstructed one $\hat{\mathbf{x}}$ is smaller than 10^{-5} , that is $\|\mathbf{x} - \hat{\mathbf{x}}\|_2 < 10^{-5}$. Figs. 2 and 3 present the reconstruction results for binary zero-one and Gaussian sparse signals respectively, which show that the reconstruction performance of the proposed method is much better than that of the SP and BP methods, with a successful reconstruction probability beyond 0.9.

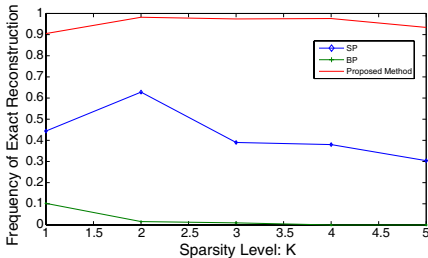


Figure 2. Frequency of exact reconstruction for the zero-one signal.

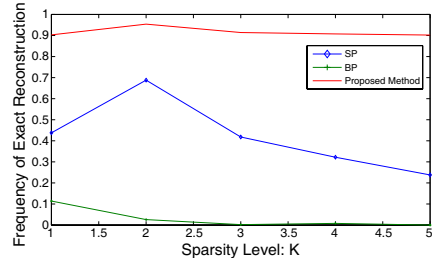


Figure 3. Frequency of exact reconstruction for the Gaussian signal.

4. COMPRESSED SENSING BASED MULTIPLE TARGET DETECTION ALGORITHM

In recent work related with compressed sensing based STAP [17–20], the coherence of the sensing matrix is not low due to the

high resolution of the DOA-Doppler plane, which does not guarantee a good reconstruction of the sparse vector with large probability. Consequently, the direct estimation of the target amplitude may be unreliable using sparse representation when locating a moving target from the surrounding strong clutter. The weak element (target) is always submerged in the prominent elements (clutter). In [20], only the prominent elements are extracted from the sparse radar scene, and an additional adaptive filter is used to suppress the clutter to identify the target.

However, in this paper, we can obtain a reconstructed radar scene with high accuracy based on the test cell using the proposed similar sensing matrix pursuit algorithm. Both the prominent elements (clutter) and the weak elements (multiple targets) can be identified accurately with the proposed method. Consequently, it is not difficult to distinguish the weak elements from the prominent elements in the reconstructed radar scene. In the following, a simple algorithm is proposed to detect multiple targets in the reconstructed radar scene.

Algorithm 2: Compressed Sensing Based Multiple Target Detection Algorithm

- (i) Use the proposed similar sensing matrix pursuit algorithm to obtain the estimate of the original sparse vector (\mathbf{x}_{test}), $\hat{\mathbf{x}}_{\text{test}}$, based on the original sensing matrix Φ , and the measurement vector \mathbf{y}_{test} (the snapshot from the test cell). The entries corresponding to noise in the original sparse vector \mathbf{x}_{test} are set as zero in $\hat{\mathbf{x}}_{\text{test}}$ according to the proposed algorithm. The nonzero elements of the reconstructed sparse vector $\hat{\mathbf{x}}_{\text{test}}$ contain the prominent elements (clutter) and the weak elements (the targets).
 - (ii) Distinguish the weak elements from the prominent elements to detect multiple targets. For each element of the estimated sparse vector, $\hat{x}_{\text{test}}(i)$, $i = 1, \dots, VD$,
 - if $|\hat{x}_{\text{test}}(i)| > T_{\text{clutter}}$
 $\hat{x}_{\text{test}}(i)$ corresponds to clutter.
 - else if $|\hat{x}_{\text{test}}(i)| > 0$
 $\hat{x}_{\text{test}}(i)$ corresponds to a target.
- end

Here T_{clutter} is a threshold set to distinguish the targets from the clutter. It is assumed that the CSR is sufficient large (> 20 dB). The clutter scatters are with much higher amplitudes than the targets. The entries of $\hat{\mathbf{x}}_{\text{test}}$ can be arranged in descend order according to their amplitudes as,

$$\begin{aligned} & |\hat{x}_{\text{test}}[1]| > |\hat{x}_{\text{test}}[2]| > \dots > |\hat{x}_{\text{test}}[k]| \\ \gg & |\hat{x}_{\text{test}}[k+1]| > \dots > |\hat{x}_{\text{test}}[NK \times VL]|, \end{aligned} \quad (28)$$

where $\hat{x}_{test}[1]$ denotes the entry that with the largest amplitude, and the similar definitions for $\hat{x}_{test}[2], \dots, \hat{x}_{test}[NK \times VL]$. The sudden change of the amplitude between $\hat{x}_{test}[k]$ and $\hat{x}_{test}[k+1]$ is caused by the large difference between the amplitudes of the clutter scatter and target element. And the value of $T_{clutter}$ is set proportional to the smallest amplitude of the clutter scatters, as $T_{clutter} = \kappa|\hat{x}_{test}[k]|$. The constant κ is drawn from the range of $[10^{-2}, 10^{-1}]$ to ensure that the targets can be distinguish from the clutter scatters accurately. The proposed algorithm can identify multiple targets directly from the reconstructed radar scene (the DOA-Doppler plane), which reduces the computing complexity efficiently.

5. SIMULATION RESULTS AND ANALYSIS

In this section, the proposed similar sensing matrix pursuit algorithm is compared with the D3SR method [20], in reconstructing sparse radar scenarios. Furthermore, the proposed algorithm is also compared with several classic STAP algorithms, e.g., the sample matrix inversion (SMI) method [14], the angle-Doppler compensation (ADC) method [33] and the D3SR method using the improvement factor loss (IF_{Loss}), which is a common metric in evaluating the performance of the STAP methods.

An airborne, side-looking radar system consisting of half-wavelength spaced ULAs is considered in this section. The radar system is comprised of 16 arrays and the data is organized in CPIs of 16 pulses. The clutter is uniformly distributed between the directions of $-80^\circ \sim 70^\circ$ and is contained in both the training cells and the test cell. The DOA-Doppler plane is divided into 200×180 square grids, where x -axis is for DOA angle and y -axis for Doppler frequency. The initial DOA angle (θ_0), the DOA angle interval ($\Delta\theta$), the initial Doppler frequency (f_{d_0}) and the Doppler frequency interval (Δf_d) equal -90° , 1° , -400 Hz and 4 Hz, respectively.

First, the proposed algorithm is compared with the D3SR method in reconstructing sparse radar scenarios in two examples. The environment setting of the first example is shown in Fig. 4, where two pairs of targets (appeared as four blue dots) are placed near the clutter ridge (appeared as a red ridge). One pair of targets are with the same Doppler frequency (-160 Hz), and their DOA angles are -25° and -20° respectively. The other pair of targets are with the same DOA angle (16°), and their Doppler frequencies are 68 Hz and 56 Hz respectively. The color represents the amplitude of the reflection coefficients (in dB). The clutter is with red color, which represents the range of $[-5, 0]$ dB from the side color bar. The target point is blue,

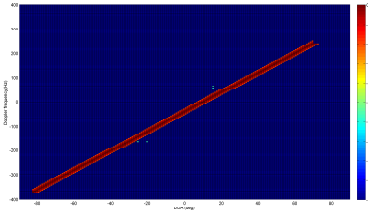


Figure 4. True sparse radar scene: four targets.

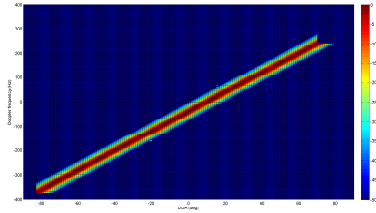


Figure 5. Estimated sparse radar scene using the D3SR method: four targets.

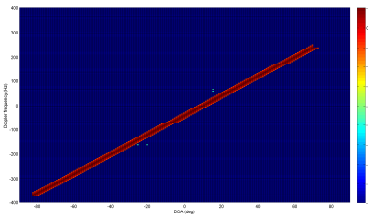


Figure 6. Estimated sparse radar scene using the proposed method: four targets.

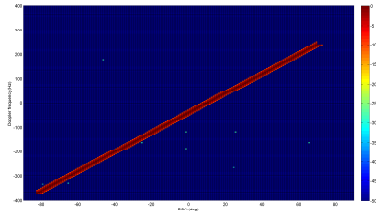


Figure 7. True sparse radar scene: ten randomly distributed targets.

which represents the range of $[-30, -25]$ dB. Therefore, the simulation setting is with a high CSR ranging from 20 to 30 dB.

The simulation results are shown in Figs. 4–6. Fig. 4 gives the actual sparse radar scene. Figs. 5, 6 provide the sparse radar scenes reconstructed by the D3SR method and the proposed method, respectively. From Fig. 5, it can be seen that the D3SR method wrongly recovers the elements near the clutter ridge besides the clutter scatters in the DOA-Doppler plane, where the targets are submerged in the wrongly recovered nearby elements. This is due to the reason that the columns in the original sensing matrix corresponding to the elements near the clutter are highly coherent (similar) with the columns corresponding to the clutter scatters. The D3SR method can not distinguish the highly coherent columns and assigns large values to their corresponding elements. However, the proposed method can estimate the weak elements (targets) as well as the prominent elements (clutter) accurately, and it can distinguish the targets from clutter successfully in the DOA-Doppler plane (Fig. 6). This verifies that the proposed similar sensing matrix pursuit method can cope with the deterministic sensing matrix with high coherence efficiently.

The second example is utilized to compare the reconstruction

performance of the two methods (the D3SR and the proposed methods) in estimating targets with different positions under different noise levels. Ten targets distributes randomly in the DOA-Doppler plane. The reconstruction error is adopted to evaluate the reconstruction performance of the two methods, which is defined as

$$\chi = \frac{\|x_{estimate} - x\|_2^2}{\|x\|_2^2}, \tag{29}$$

where x and $x_{estimate}$ represent the true and estimated signal representing the sparse radar scene respectively. For a given signal-noise-ratio (SNR), we make 100 trails Monte Carlo simulations (indicated by N_{MC}). In each trail, the locations of ten targets are randomly distributed in the DOA-Doppler plane. Figs. 7–9 show the simulation results from one trial with SNR equaling 20 dB. In Fig. 8, the targets near the clutter ridge are submerged in the wrongly

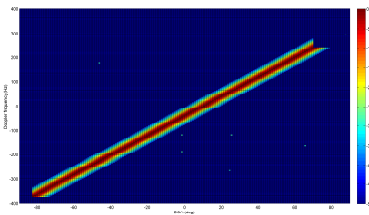


Figure 8. Estimated sparse radar scene using the D3SR method: ten randomly distributed targets.

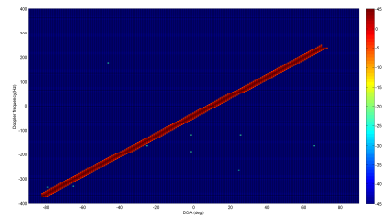


Figure 9. Estimated sparse radar scene using the proposed method: ten randomly distributed targets.

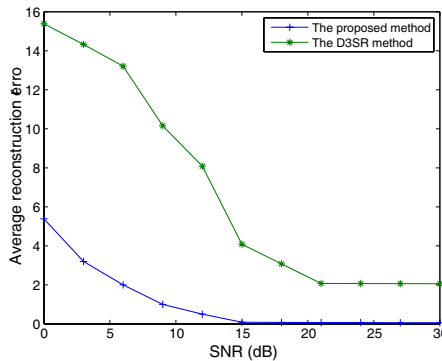


Figure 10. Reconstruction performance (average reconstruction error) of the proposed method and the D3SR method with varying SNRs.

reconstructed nearby elements when using the D3SR method, while the proposed method can estimate the weak elements (targets) as well as the prominent elements (clutter) accurately (Fig. 9). Fig. 10 indicates the variation of average reconstruction error ($\chi_{average} = \sum_{i=1}^{N_{MC}} \chi^i / N_{MC}$) with SNR varying from 0 dB to 30 dB, which shows that the proposed method is resilient to the measurement noise. The proposed algorithm can do perfect detection (< 0.1) of ten targets with measurement noise when the SNR is above 20 dB. For the D3SR method, large reconstruction error (> 2) exists even when the SNR exceeds 20 dB.

Moreover, the proposed algorithm is compared with several classic STAP algorithms, e.g., the SMI method, the ADC method and the D3SR method, using the improvement factor loss, which is defined as [34],

$$IF_{Loss} = \frac{SCR_{out}/SCR_{in}}{(SCR_{out}/SCR_{in})_{opt}}, \quad (30)$$

where SCR_{out} and SCR_{in} denote the output signal-clutter-ratio (SCR) and input SCR, respectively. A classic simulation setup in STAP simulations is adopted, where a moving target is coming with a DOA angle of 20° . Different output SCRs are then considered with varying Doppler frequencies. Fig. 11 gives the IF_{Loss} performance of different STAP algorithms. Because the SCR improvement is mostly achieved in the subspace orthogonal to the clutter, all the STAP methods (the SMI, ADC and D3SR methods) suffer considerable degradation near the clutter notch, no matter what size the total space (i.e., system DOF) is. However, the proposed similar sensing matrix pursuit algorithm detects the target directly based on the reconstructed radar scene, and it achieves the comparable performance with the optimal filter.

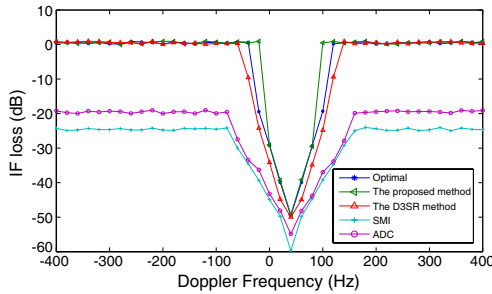


Figure 11. IF_{Loss} performance of different STAP methods at a DOA angle of 20° as a function of the Doppler frequency.

6. CONCLUSION

In this paper, a novel compressed sensing based method, the similar sensing matrix pursuit, is proposed to detect unknown moving targets in strong clutter situation directly on the test cell, which largely reduces the computing complexity. From the simulation results, it can be seen that the proposed method can estimate the weak elements (targets) as well as the prominent elements (clutter) accurately, and it can distinguish the targets from clutter successfully in the sparse radar scene (the DOA-Doppler plane).

ACKNOWLEDGMENT

This work was supported by the National Natural Science Foundations of China (No. 61104051, No. 61074176 and No. 61004087), the Fundamental Research Funds for the Central Universities, and the Scientific Research Foundation for the Returned Overseas Chinese Scholars, State Education Ministry.

REFERENCES

1. Baraniuk, R. and P. Steeghs, "Compressive radar imaging," *Proc. Radar Conference*, 128–133, 2007.
2. Liu, Z., X. Wei, and X. Li, "Adaptive clutter suppression for airborne random pulse repetition interval radar based on compressed sensing," *Progress In Electromagnetics Research*, Vol. 128, 291–311, 2012.
3. Yang, M. and G. Zhang, "Parameter identifiability of monostatic MIMO chaotic radar using compressed sensing," *Progress In Electromagnetics Research B*, Vol. 44, 367–382, 2012.
4. Liu, J., X. Li, S. Xu, and Z. Zhuang, "ISAR imaging of non-uniform rotation targets with limited pulses via compressed sensing," *Progress In Electromagnetics Research B*, Vol. 41, 285–305, 2012.
5. Wei, S. J., X.-L. Zhang, J. Shi, and K. F. Liao, "Sparse array microwave 3-D imaging: Compressed sensing recovery and experimental study," *Progress In Electromagnetics Research*, Vol. 135, 161–181, 2013.
6. Li, J., S. Zhang, and J. Chang, "Applications of compressed sensing for multiple transmitters multiple azimuth beams SAR imaging," *Progress In Electromagnetics Research*, Vol. 127, 259–275, 2012.

7. Chen, J., J. Gao, Y. Zhu, W. Yang, and P. Wang, "A novel image formation algorithm for high-resolution wide-swath spaceborne SAR using compressed sensing on azimuth displacement phase center antenna," *Progress In Electromagnetics Research*, Vol. 125, 527–543, 2012.
8. Wei, S. J., X.-L. Zhang, and J. Shi, "Linear array SAR imaging via compressed sensing," *Progress In Electromagnetics Research*, Vol. 117, 299–319, 2011.
9. Wei, S. J., X.-L. Zhang, J. Shi, and G. Xiang, "Sparse reconstruction for SAR imaging based on compressed sensing," *Progress In Electromagnetics Research*, Vol. 109, 63–81, 2010.
10. Gong, Q. and Z.-D. Zhu, "Study stap algorithm on interference target detect under nonhomogenous environment," *Progress In Electromagnetics Research*, Vol. 99, 211–224, 2009.
11. Tounsi, M. L., R. Touhami, A. Khodja, and M. C. E. Yagoub, "Analysis of the mixed coupling in bilateral microwave circuits including anisotropy for MICS and MMICS applications," *Progress In Electromagnetics Research*, Vol. 62, 281–315, 2006.
12. Asadi, S. and M. C. E. Yagoub, "Efficient time-domain noise modeling approach for millimeter-wave fets," *Progress In Electromagnetics Research*, Vol. 107, 129–146, 2010.
13. Habib, M. A., A. Bostani, A. Djaiz, M. Nedil, M. C. E. Yagoub, and T. A. Denidni "Ultra wideband CPW-FED aperture antenna with WLAN band rejection," *Progress In Electromagnetics Research*, Vol. 106, 17–31, 2010.
14. Guerci, J., *Space-time Adaptive Processing for Radar*, Artech House, 2003.
15. Klemm, R., "Applications of space-time adaptive processing," *Inspec/IEE*, 2004.
16. Melvin, W., "A STAP overview," *IEEE Aerospace and Electronic Systems Magazine*, Vol. 19, No. 1, 19–35, 2004.
17. Zhang, H., G. Li, and H. Meng, "A class of novel STAP algorithms using sparse recovery technique," *Information Theory*, Arxiv preprint arXiv: 0904.1313, 2009.
18. Selesnick, I. W., S. U. Pillai, K. Y. Li, and B. Himed, "Angle-Doppler processing using sparse regularization," *Proc. IEEE International Conference on Acoustics, Speech and Signal Processing*, 2750–2753, 2010.
19. Parker, J. and L. Potter, "A Bayesian perspective on sparse regularization for STAP post-processing," *IEEE Radar Conference*, 1471–1475, 2010.

20. Sun, K., H. Meng, and Y. Wang, "Direct data domain STAP using sparse representation of clutter spectrum," *Signal Processing*, Vol. 91, No. 9, 2222–2236, 2011.
21. Donoho, D. L. and M. Elad, "Optimally sparse representation in general (nonorthogonal) dictionaries via l_1 minimization," *Proc. Nat. Acad. Sci.*, Vol. 100, No. 5, 2197–2202, 2003.
22. Gribonval, R. and M. Nielsen, "Sparse representations in unions of bases," *IEEE Trans. on Information Theory*, Vol. 49, No. 12, 3320–3325, 2003.
23. Tropp, J. A., "Greed is good: Algorithmic results for sparse approximation," *IEEE Trans. on Information Theory*, Vol. 50, No. 10, 2231–2242, 2004.
24. Donoho, D., "Compressed sensing," *IEEE Trans. on Information Theory*, Vol. 52, No. 4, 1289–1306, 2006.
25. Ben-Haim, Z., Y. C. Eldar, and M. Elad, "Coherence-based performance guarantees for estimating a sparse vector under random noise," *IEEE Trans. on Signal Processing*, Vol. 58, No. 10, 5030–5043, 2010.
26. Duarte, M. F. and Y. C. Eldar, "Structured compressed sensing: From theory to applications," *IEEE Trans. on Signal Processing*, Vol. 59, No. 9, 4053–4085, 2011.
27. Dai, W. and O. Milenkovic, "Subspace pursuit for compressive sensing signal reconstruction," *IEEE Trans. on Information Theory*, Vol. 55, No. 5, 2230–2249, 2009.
28. Stojanovic, I., W. Karl, and M. Cetin, "Compressed sensing of mono-static and multi-static SAR, SPIE defense and security symposium," *Algorithms for Synthetic Aperture Radar Imagery XVI*, Orlando, Florida, 2009.
29. Joachim H. G. E., "On compressive sensing applied to radar," *Signal Processing*, Vol. 90, No. 5, 1402–1414, 2010.
30. Donoho, D. L., M. Elad, and V. N. Temlyakov, "Stable recovery of sparse overcomplete representations in the presence of noise," *IEEE Trans. on Information Theory*, Vol. 52, No. 1, 6–18, 2006.
31. Elad, M., "Optimized projections for compressed sensing," *IEEE Trans. on Signal Processing*, Vol. 55, No. 12, 5695–5702, 2007.
32. SparseLab [Online]. Available: <http://dsp.rice.edu/cs>.
33. Himed, B., Y. Zhang, and A. Hajjari, "STAP with angle-Doppler compensation for bistatic airborne radars," *Proc. of IEEE National Radar Conference*, 22–25, Long Beach, California, 2002.
34. Klemm, R., *Principles of Space-time Adaptive Processing*, IEE Press, 1999.